Development 116, 953-966 (1992)
Printed in Great Britain © The Company of Biologists Limited 1992

Increased levels of the *Drosophila* Abelson tyrosine kinase in nerves and muscles: subcellular localization and mutant phenotypes imply a role in cell-cell interactions

RANDY L. BENNETT and F. MICHAEL HOFFMANN*

McArdle Laboratory for Cancer Research, University of Wisconsin, Madison, Wisconsin 53706, USA

*Author for correspondence

Summary

Mutations in the *Drosophila* Abelson tyrosine kinase have pleiotropic effects late in development that lead to pupal lethality or adults with a reduced life span, reduced fecundity and rough eyes. We have examined the expression of the abl protein throughout embryonic and pupal development and analyzed mutant phenotypes in some of the tissues expressing *abl*. abl protein, present in all cells of the early embryo as the product of maternally contributed mRNA, transiently localizes to the region below the plasma membrane cleavage furrows as cellularization initiates. The function of this expression is not yet known. Zygotic expression of abl is first detected in the post-mitotic cells of the developing muscles and nervous system midway through embryogenesis. In later larval and pupal stages, abl protein levels are also highest in differentiating muscle and neural tissue including the photoreceptor cells of the eye. abl protein is localized subcellularly to the axons of the central nervous system, the embryonic somatic muscle attachment sites and the apical cell junctions of the imaginal disk epithelium. Evidence for abl function was obtained by analysis of mutant phenotypes in the embryonic somatic muscles and the eye imaginal disk. The expression patterns and mutant phenotypes indicate a role for *abl* in establishing and maintaining cell-cell interactions.

Key words: Abelson tyrosine kinase, *Drosophila*, eye development, muscle development, expression, *disabled*, cell-cell interaction, nervous system.

Introduction

Cytoplasmic protein-tyrosine kinases (PTKs) were first identified as the transforming proteins of several acutely oncogenic retroviruses (Collett and Erikson, 1978; Hunter and Sefton, 1980; Witte et al., 1980). One of these, the Abelson tyrosine kinase, is the transforming protein of the Abelson murine leukemia virus in mice and the Philadelphia chromosome in humans (Witte, 1986). Although much is known about the oncogenic activation of the Abelson kinases (reviewed by Daley and Ben-Neriah, 1991), little is known about the biochemical pathways through which the transforming forms of the Abelson kinase lead to neoplastic transformation. Similarly, little is known about the functions of the non-oncogenic, cellular forms of PTKs that are expressed in diverse tissues at many times during development, and have been implicated in normal cellular and developmental processes (Adamson, 1987; Hanley, 1988). To gain a better understanding of the functions of Abelson-like PTKs in development, we have undertaken a developmental genetic and molecular study of the Abelson tyrosine kinase gene (*abl*) in *Drosophila melanogaster* (Henkemeyer et al., 1987, 1988, 1990; Gertler et al., 1989, 1990; Holland et al., 1990; Hoffmann, 1991).

The *Drosophila* and mammalian abl proteins are well conserved in regions believed to be important for kinase activity and regulation. *Drosophila* abl is approximately 80% similar to the vertebrate c-abl proteins in the src-homology 2(SH2), src-homology 3(SH3) and kinase domains (Henkemeyer et al., 1988). Like the type IV (mouse) and 1b (human) forms of the c-abl proteins, *Drosophila* abl contains an amino-terminal glycine, which in the mammalian proteins is a site for myristylation. There is, however, little conservation of *Drosophila* abl in the mammalian c-abl carboxy-terminal domain (24% identity; Henkemeyer et al., 1988). A second member of the Abelson family cloned from human cells is the Abelson related gene (*arg*; Kruh et al., 1990; Perego et al., 1991). *Drosophila* abl is equally similar to the mammalian arg and c-abl proteins in the SH2, SH3 and kinase domains (Kruh et al., 1990). In the carboxy-terminal domain, the *Drosophila* abl and human arg proteins share a statistically significant 30% identity in alignments generated by the GCG Bestfit program (Devereaux et al., 1984; F. Gertler, unpublished observations).

Mutations in the *abl* gene of *Drosophila* lead to developmental defects that appear late in development. These include: pupal lethality as pharate adults, reduced fecundity, a shortened life span and rough eyes (Henkemeyer et al., 1987). Paralleling these results in *Drosophila*, gene disruptions of murine c-*abl* lead to pleiotropic defects late in development (Shwartzberg et al., 1991; Tybulewitz, et al., 1991). Multiple mutant alleles of three different genes that enhance the *Drosophila abl* mutant phenotypes have been isolated (Gertler et al., 1989; Hoffmann, unpublished observations). When *abl* mutant animals are heterozygous for mutations in any of these genes, the lethal phase is shifted from late pupal/early adult stages to embryonic/larval stages. The earlier lethality is associated with the appearance of visible defects in the axonal architecture of the embryonic central nervous system (CNS). In addition, three mutations that suppress the *abl* mutant phenotypes have also been isolated, all of which map to the gene *enabled* (*ena*; Gertler et al., 1990). Understanding the molecular basis for these genetic interactions is a primary goal in our laboratory.

We have previously shown that the *Drosophila* abl protein is expressed at higher levels in the axons of the developing CNS during *Drosophila* embryogenesis (Gertler et al., 1989). Consistent with this axonal expression, genetic interactions with *disabled* (dab) and *fasciclin I* (*fas I*) indicate that *abl* is involved in axonogenesis and axon pathfinding (Gertler et al., 1989; Elkins et al., 1990). Proper localization of abl to the axonal compartment of the neuronal cells correlates with the ability of the abl protein to carry out its functions (Henkemeyer et al., 1990). In this report, we present a detailed description of the localization of the abl protein during embryogenesis and pupal development of *Drosophila melanogaster*. We have generated a more sensitive antibody to the abl protein and demonstrate that the expression of *abl* is more diverse and dynamic during *Drosophila* development than previously reported. We also show that the abl protein is localized to specialized regions of cell-cell interactions and report on the *abl*-dependent mutant phenotypes in the developing embryonic muscle and adult eye.

Materials and methods

Production of abl antibodies

Antibodies to abl were raised against the β-galactosidase-Abelson bacterial fusion protein, pURABLkin (Henkemeyer et al., 1988). This fusion protein contains the SH3, SH2 and kinase domains of abl. Fusion protein was produced and purified as described in Gertler et al. (1989). Briefly, inclusion bodies were isolated by the method of Nagai et al. (1985), except large molecular mass DNA was sheared using a polytron rather than incubating lysates with DNaseI in the presence of divalent cations. Inclusion bodies were then homogenized in 2× SDS sample buffer (Laemmli, 1970) and fractionated by electrophoresis on a preparative 5% polyacrylamide gel (Laemmli, 1970). The preparative gel was stained with an aqueous Commassie stain (0.6% Brilliant Blue R, Sigma Chemical Co., 20% Methanol, 16 mM Tris-HCl [pH 7.5]). The protein band corresponding to the ABLkin fusion protein was excised. For immunizations, New Zealand White rabbits (New Franken) were immunized with a polyacrylamide gel slice containing approximately 500 μg of fusion protein homogenized in Freunds incomplete adjuvant (Sigma Chemical Co.). Rabbits were injected on days 1, 14, and 21 followed by monthly boosts. For affinity purification of anti-ablkin antibodies, 10 mg ABLkin protein was electroeluted using an Elutrap (Schleicher and Schuell), dialyzed against 0.01 M Hepes buffer (N-(2-Hydroxyethyl)piperazine-N′-(2-ethanesulfonic acid)), pH 8.0 and coupled to a mixed bed of Affigel 10 and Affigel 15 (BioRad) at 1 mg/ml column bed according to manufacturer's directions. For removal of anti-β-galactosidase antibodies, 50 mg of β-galactosidase was coupled to Affigel 10 in 0.01 M Hepes buffer (2 mg/ml column bed). Antiserum was passed over the β-galactosidase column until no immunoreactivity in the flowthrough was detected on dot blots (1 μg/spot) of a second β-galactosidase-abl fusion protein, pURABLcarb (Henkemeyer et al., 1988). Antibodies to abl were then affinity purified by passing the antiserum over the ABLkin column. The column was washed thoroughly (until $A_{280} < 0.01$) with phosphate-buffered saline (PBS, 6.13 mM K_2HPO_4, 3.87 mM KH_2PO_4, 140 mM NaCl [pH 7.0-7.2]), followed by washes with borate-buffered saline (1 M NaCl, 0.1 M boric acid, 0.025 M sodium borate [pH 8.3]) containing 0.1% Tween-20. The column was then equilibrated with 10 mM sodium phosphate buffer (pH 7.2) prior to elution with 0.1 M glycine (pH 3.0). 1 ml fractions were collected into 200 μl of 1.0 M Tris-HCl (pH 8.0). Peak fractions were pooled and tested for specificity for the abl portion of the fusion protein using dot blots of ABLcarb (Henkemeyer et al., 1988) and ABLkin. The affinity purified antibodies (anti-ablkin) could readily detect 5 ng of ABLkin fusion protein; no immunoreactivity was detected against 1 μg of ABLcarb fusion protein (data not shown). Antibodies raised in rabbits to abl, using the β-galactosidase-Abelson fusion protein ABLkin, were found to be approximately 20- to 50-fold more sensitive when assayed on dot blots of fusion proteins than the anti-ablcarb antibodies used in previous studies (data not shown).

Immunoprecipitations and western blot analysis

Protein extracts were prepared 0-24 hours postpuparium formation (ppf) from wild-type pupae (Canton S), *abl* null pupae (*ena*^{210}/+; *Df(3L)std11*/*Df(3L)stj7*) and pupae containing *abl* point mutant alleles (*abl*^{1}, *abl*^{2}, *abl*^{3}, *abl*^{4} or *abl*^{5}/*Df(3L)stj7*) as described in Henkemeyer et al. (1990). Briefly, 100 pupae were homogenized in 2 ml of IP buffer (1% Triton X-100, 10 mM Tris-HCl [pH 7.6], 10 mM EDTA, 50 mM NaCl, 30 mM sodium pyrophosphate, 0.1 % NaN_3) supplemented with a protease inhibitor cocktail (2 mM PMSF, 20 μg/ml, leupeptin, 20 μg/ml pepstatin, 20 μg/ml aprotinin; Boehringer Mannheim) and 1 mg/ml bovine serum albumin (BSA, Sigma Chemical Co.). Extracts were clarified by centrifugation in a microfuge at 12,000 ***g*** at 4°C. 1 ml of each extract was incubated with 2 μg of anti-ablkin at 4°C for 2 hours, followed by incubation with 50 μl of protein-A agarose (Sigma Chemical Co.) for 2 hours at 4°C. Precipitates were washed at room temperature 3 times in IP buffer with protease inhibitors and BSA, followed by 3 washes in IP buffer with protease inhibitors without BSA, and then boiled in 50 μl 2× SDS-sample buffer (Laemmli, 1970). Proteins were resolved on an 8% polyacrylamide gel (Laemmli, 1970) and electrotransferred to nitrocellulose (400 mA for 8 hours at 4°C) in 25 mM Tris base, 20 mM glycine and 20% methanol. The nitrocellulose membrane was blocked with Blotto (1× PBS, 1% Carnation instant non-fat dry milk, 0.5% Tween-20; Johnson et al., 1984). After blocking for 1 hour, the nitrocellulose membrane was incubated with anti-ablkin at 0.4 μg/ml in Blotto for 1 hour. The blot was washed for 30 minutes with Blotto and then incubated with goat anti-rabbit IgG conjugated to alkaline phosphatase (Sigma Chemical Co.) diluted 1:1000 in Blotto from the manufacturer's stock concentration. The blot was washed for 30 min-

utes in Blotto, followed by a brief rinse in 0.1 M Tris (pH 9.4). Immunoreactive proteins were visualized using 1.2 mg/ml nitro blue tetrazolium and 25 μg/ml bromochloroindolylphosphate (Sigma Chemical Co.) in 0.1 M Tris (pH 9.6), 0.1 M NaCl, and 5 mM $MgCl_2$. This procedure detected the anti-ablkin immunoglobulin heavy chain at 48×10^3 M_r. No protein bands were observed at 48×10^3 M_r when ^{125}I-labeled protein A was used to detect immunoreactive proteins on the western blots (data not shown). We concluded from this observation that the presence of the anti-ablkin heavy chain did not mask the presence of abl proteins in this size range.

Whole-mount RNA in situs

A 2.8 kb *Eco*RI fragment from the *abl* cDNA P1 and a 1.2 kb *Eco*RI/*Bgl*II fragment from the *abl* cDNA L (Henkemeyer et al., 1988) were labeled with digoxigenin using the modified method of Tautz and Pfeiffle (1989) described by Masucci et al. (1990). Embryos were fixed and probed with the labeled *abl* cDNA fragments using the method of Tautz and Pfeiffle (1989), except hybridization was extended to 36 hours, washes after hybridization were extended to overnight (12-14 hours) and washes after the incubation with anti-digoxigenin antibody were extended to 8 hours. These extended washes generally reduced background staining.

Immunostaining

Embryos were collected and prepared for immunostaining as previously described (Gertler et al., 1989), except that 100% methanol was used to remove the vitelline membrane from the embryos. Embryos were staged using the conventions established by Campos-Ortega and Hartenstein (1985). Embryos were blocked for several hours in PBT (PBS containing 2% BSA, 0.1% Triton X-100) containing 5% normal goat serum (PBT+NGS). Embryos were incubated in primary antibody (anti-ablkin) diluted to 0.3 μg/ml in PBT+NGS overnight at 4°C. Embryos were washed for 12 hours at 4°C with several changes of PBT (at least 10). PBT+NGS was added to the last wash to block embryos prior to the addition of the secondary antibody. The secondary antibody (biotinylated goat anti-rabbit, Vector labs) was added to the embryos at a concentration of 2.5 μg/ml in 1 ml of PBT+NGS. Embryos were incubated for 8 hours at 4°C. The embryos were then washed for 8 hours at 4°C with several changes of PBT. NGS was added to the last wash. The embryos were then incubated for 4 hours at 4°C in streptavidin-conjugated horseradish peroxidase (HRP) diluted 1:300 from the supplier's concentration (Immunoselect, Bethesda Research Labs) in PBT+NGS. Embryos were washed for 4 hours with several changes of PBT. Embryos were rinsed once in TBS (50 mM Tris-HCl [pH 7.5], 150 mM NaCl), and then stained in HRP reaction buffer (1× TBS, 0.003% H_2O_2, 0.5 mg/ml 3,3′-diaminobenzidine, Sigma Chemical Co.) for 15 minutes. The reaction was stopped by flooding the embryos with PBT containing 0.2% NaN_3. After several washes in PBT, followed by several washes in PBS, embryos were dehydrated through an ethanol series and cleared in methyl salicylate. Embryos (and all HRP-stained tissues) were examined using differential interference contrast optics on a Zeiss Axiophot microscope.

To obtain embryos that did not express the abl protein, females containing deletions overlapping in *abl* and containing an allele of the suppressor of *abl*, *enabled* (*ena*$^{2.10}$/+; *Df(3L)std11*/*Df(3L)stE36*), were crossed to males that contained an *abl* deletion heterozygous with a tandem duplication covering the *abl* gene, *Df(3L)stE36*/*Dp(3;3)st*$^+$*g18*. In this cross there is no maternal expression and 50% of the embryos are also without zygotic expression. The duplication was used to increase the level of paternally inherited abl expression.

To examine the phenotype of embryonic muscles, embryos were stained with both anti-ablkin and anti-myosin 722 antibody (provided by Dr Daniel Kiehart, Harvard University) by the method described above. Anti-myosin 722 antibodies were used at a 1:500 dilution of the stock provided. *abl dab* double mutant embryos were derived from a cross of *Df(3L)stj7*, *dab*^{m2}/TM6B (females) × *Df(3L)std11*/TM6B (males). Mutant embryos were identified as those that failed to show axon staining in the CNS with the anti-ablkin antibody.

Larvae and pupae were dissected in PBS and fixed in 4% paraformaldehyde in PBS for 30 minutes at room temperature. Late pupal tissues (24 hours ppf or older) were fixed overnight (12-16 hours) at 4°C. Following fixation, tissues were washed three times in PBS followed by incubation in PBS containing 0.3% H_2O_2 for 5 minutes. Tissues were washed again three times in PBS (5 minutes each), followed by two washes in PBS containing 0.1% Triton X-100, and then placed in PBT for three hours at 4°C. All subsequent treatments were performed at 4°C. Prior to primary antibody incubation, tissues were placed in PBT+NGS for 2 hours. Transfer of tissues through the washes and incubations was facilitated by using nitex mesh baskets. For the disk staining, anti-ablkin was pre-absorbed against imaginal disk/brain complexes dissected from pupae null for the abl protein (approximately 20-30) at 5 μg/ml overnight. Tissues were incubated with anti-ablkin at 0.2 μg/ml in PBT+NGS overnight (12-14 hours). Tissues were washed with several changes (at least 12 changes) of PBT for 18 hours with slight agitation. Tissues were then incubated in biotinylated goat anti-rabbit IgG (1 μg/ml in PBT+NGS) for 8 hours, followed by extensive washes with PBT (at least 12 changes) for 12-14 hours (overnight). Tissues were then incubated in streptavidin-HRP diluted 1:500 in PBT+NGS for 4 hours. Following 4 hours of washes in PBT (at least 10 changes), tissues were rinsed in TBS and reacted in HRP reaction buffer for 15 minutes. Imaginal tissues were cleared in glycerol and mounted in Aqua-polymount (Polysciences) for whole-mount viewing or dehydrated in ethanol, cleared in methyl salicylate and mounted in Epon-Araldite for sectioning (See below).

To generate larvae and pupae that did not express the abl protein, *ena*$^{2.10}$/CyO; *Df(3L)std11*/TM6,B males were crossed to *Df(3L)stE36*/TM6,B females. The TM6,B balancer carries the dominant larval/pupal marker *Tubby*. *abl* null larvae (*Tubby*$^+$) were picked and either dissected or aged to the appropriate pupal stage. Pupal stages are in hours from white puparium formation (hours postpuparium formation, ppf) at 25°C.

To examine phenotypes in *abl* mutant eye imaginal disks, *abl* mutant (*abl*^{4}/*Df(3L)stE36*) disks were stained with monoclonal antibody (mAb) BP104 (provided by Dr Corey Goodman, University of California, Berkeley), which specifically stains the developing photoreceptor cells of the eye imaginal disk (Hortsch et al., 1990). Dissections and stainings were performed as described above except 0.1% saponin was used in place of Triton X-100. mAbBP104 was used at a 1:3 dilution of the hybridoma supernatant. Goat anti-mouse IgG conjugated to lissamine rhodamine (Boehringer Mannheim), diluted 1:50, was used to detect mAbBP104 staining. Images were collected using a Bio-Rad MRC600 laser-scanning confocal system.

To determine when photoreceptor cell specific expression of the abl protein began, wild-type imaginal disks were double labeled with anti-ablkin and the sensory neuron specific mAb, 22C10 (Fujita et al., 1982) as described for mAbBP104. Anti-ablkin was used at 0.2 μg/ml and mAb22C210 was used at a 1:3 dilution from a hybridoma supernatant (provided by Dr Tadmiri Venkatesh, University of Oregon, Eugene). mAb22C10 was detected using a goat anti-mouse IgG conjugated to lissamine rhodamine (Boehringer Mannheim) diluted 1:50; anti-ablkin was detected using a goat anti-rabbit IgG conjugated to fluorescein isothiocyanate (Sigma Chemical Co.) diluted 1:50. Disks were

analyzed using the BioRad MRC600 laser-scanning confocal system.

Sectioning of immunostained embryos and disks

Embryos and disks were dehydrated through an ethanol series, equilibrated with methyl salicylate, washed once with methyl salicylate, and infiltrated with Epon-Araldite (26.3%(w/w) Epox 812, 19.1%(w/w) Araldite 506, 52.4%(w/w) dodecenyl succinic anhydride, 2%(w/w) Tris-dimethylaminomethyl phenol, Ernest F. Fullum Co.). Embryos and disks were then embedded in Epon-Araldite between two glass slides supported by no. 1 coverslips. One slide was treated with Teflon to permit easy removal. Selected embryos and disks were excised from the slide, oriented and glued to an Epon-Araldite block with Elmer's super fast epoxy cement. Alternatively, samples were excised from the slide and re-embedded in Epon-Aralidite in a tapered end flat mold in the proper orientation. 6 μm sections were cut using a glass knife on a Reichert-Jung Ultracut E ultramicrotome or Porter-Blum MT-2 ultra-microtome. Sections were floated on a drop of water on a glass slide, allowed to dry on a 65°C slide warmer and mounted under Permount (Fisher Scientific).

Results

Characterization of abl mutant proteins with anti-ablkin

The anti-ablkin antibodies were assayed on western blots to determine their specificity for the *abl* protein. Whole pupal lysates were prepared from wild-type pupae, pupae that were null for the *abl* protein (heterozygous for two deletions which overlap only in *abl*, *Df(3L)std11*/*Df(3L)stE36*) and pupae containing each of the five *abl* point alleles heterozygous with an *abl* deletion (*abl*^{1}, *abl*^{2}, *abl*^{3}, *abl*^{4} or *abl*^{5}/*Df(3L)stE36*). These lysates were immunoprecipitated with anti-ablkin, fractionated by SDS-PAGE, transferred to nitrocellulose and probed with anti-ablkin (Fig. 1). In the wild-type pupal lysates, anti-ablkin precipitated and detected a protein doublet migrating at approximately 180×10^3 M_r, as well as many smaller proteins believed to be degradation products of the abl protein (Fig. 1, lane 1). No immunoreactive protein bands were immunoprecipitated from the *abl* null pupal lysates (Fig. 1, lane 2). The anti-ablkin antibody, therefore, was specific for the product of the *abl* gene under the conditions of these western blots. Interestingly, immunoreactive proteins were detected in lysates from all five of the *abl* point mutant alleles. Lysates prepared from *abl*^{1}, *abl*^{2}, *abl*^{3}, and *abl*^{5} pupae contained distinct immunoreactive protein doublets ranging from 48 to 75×10^3 M_r (Fig. 1, lanes 3, 4, 5 and 6). In lysates from *abl*^{4} pupae, anti-ablkin detected several small (between 25 and 35×10^3 M_r), faint immunoreactive protein bands, making the *abl*^{4} mutation closest to being a protein null (Fig. 1, lane 7).

Expression of the abl protein from maternally derived mRNA

Using a genetic suppressor mutation in the gene *enabled* that rescues the *abl* mutant phenotypes (Gertler et al., 1990), we obtained *abl* mRNA and protein null animals at all stages of development including embryos null for the maternal contribution of *abl*. *abl* null animals were used as controls to ascertain the specificity of the observed staining for *abl* expression. It has been reported that *abl* mRNA is contributed maternally to the embryo (Wadsworth et al., 1985). RNA in situ hybridization detected *abl* mRNA distributed throughout the preblastoderm embryo (Fig. 2A,C). Negligible staining was detected in preblastoderm embryos derived from *abl* null mothers (Fig. 2B,D). The level of staining detected by RNA in situ hybridization remained constant through cellularization of the blastoderm (Fig. 2E wild type). By early gastrulation, the level of staining observed in embryos derived from wild-type mothers decreased to the levels of background staining observed in embryos derived from *abl* null mothers (compare 2G, wild type, with 2B,D,F and I, *abl* null). *abl* mRNA was not detected during germ band extension in any of the embryos derived from *abl* null mothers (compare Fig. 2H, wild type, with 2I, *abl* null). Since 50% of the embryos from the mating inherited a wild-type *abl* allele from their fathers, this indicated that no detectable zygotic expression of the *abl* gene occurred until after germ band extension.

In contrast to the *abl* mRNA, the abl protein was not maternally supplied to the oocyte. Embryos derived from wild-type and *abl* null mothers showed similar levels of background staining with anti-ablkin through the second

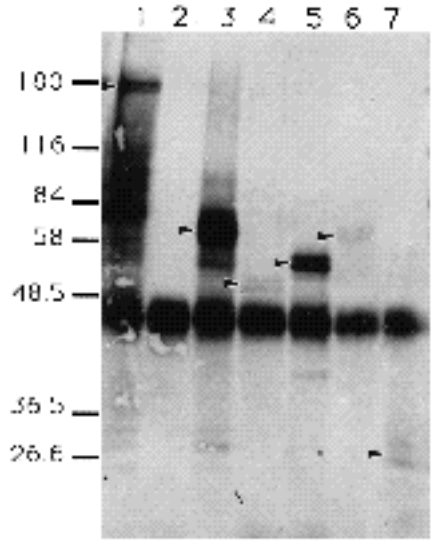

Fig. 1. Western blot analysis of wild-type and mutant abl proteins. Anti-ablkin was used to immunoprecipitate proteins from lysates of equal numbers of wild-type (Lane 1) and *abl* mutant (Lanes 2-7) pupae (0-24 hours ppf). Immunoprecipitates were analyzed on western blots using anti-ablkin as the probe. The strong band at 48×10^3 M_r, present in all lanes, corresponded to the heavy chain of the anti-ablkin IgG. The wild-type abl protein migrated at 175-180×10^3 M_r (Lane 1). Anti-ablkin did not cross react with proteins in immunoprecipitates from *abl* null pupae (Lane 2). All five of the *abl* point mutant alleles produced anti-ablkin cross-reactive proteins of altered sizes: abl^1 proteins migrated at 65 and 70×10^3 M_r (Lane 3), abl^2 proteins migrated at 51 and 53×10^3 M_r (Lane 4), abl^3 proteins migrated at 55 and 58×10^3 M_r (Lane 5) and abl^5 proteins migrated at 65 and 70×10^3 M_r (Lane 6). Several small (25-35×10^3 M_r), faint immunoreactive protein bands were observed in *abl*^{4} pupal lysates (Lane 7). Note that the wild-type and all of abl mutant proteins, except those from abl^4 pupae, ran as doublets.

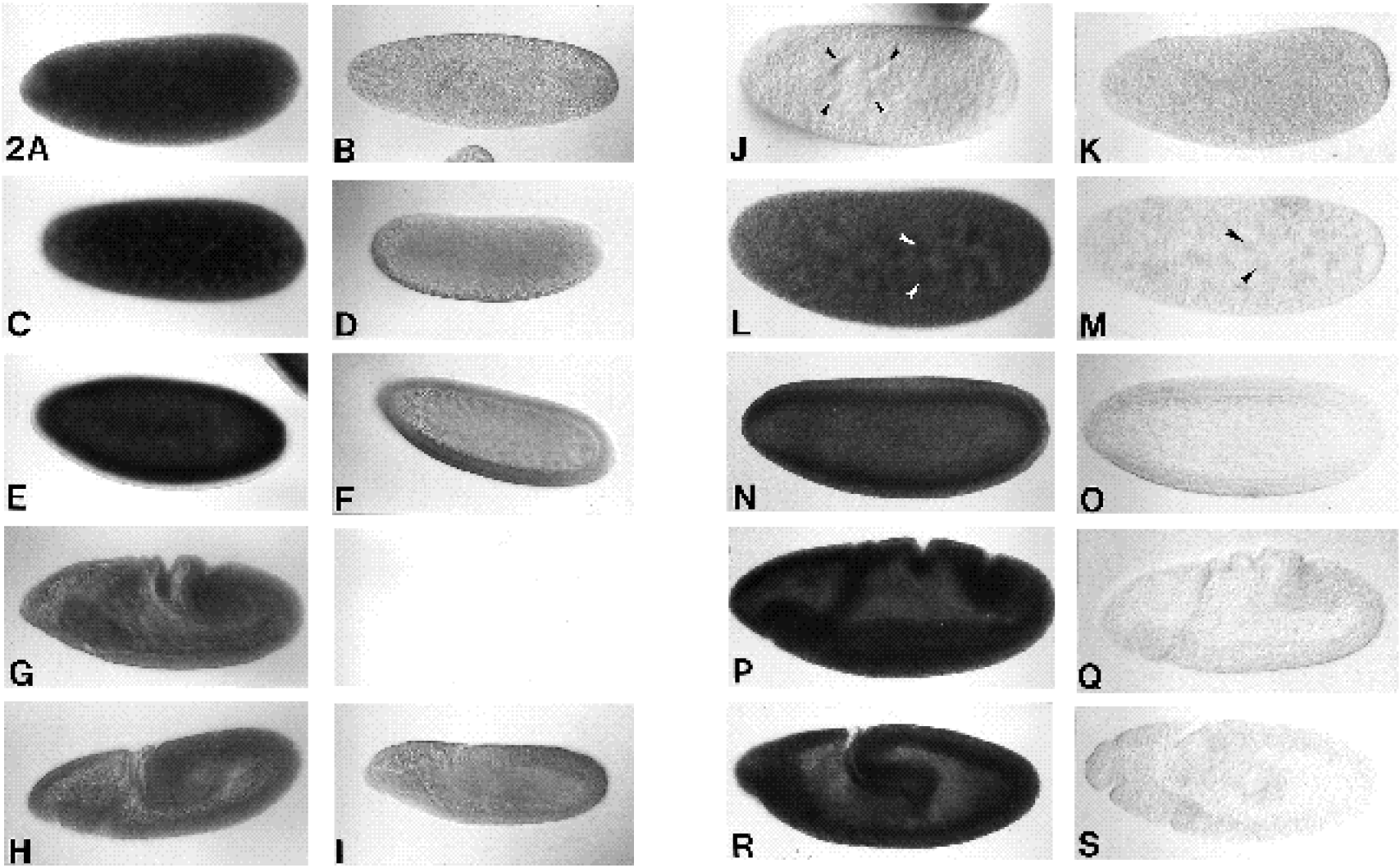

Fig. 2. Maternally derived *abl* mRNA and protein in early embryos. Wild-type and maternal *abl* null embryos were probed with digoxigenin-labeled *abl* cDNAs to detect *abl* mRNA (A-I) or with anti-ablkin to detect abl protein (J-S). Embryos are shown anterior to the left and dorsal to the top. Maternal *abl* null embryos at equivalent stages were used to indicate background levels of staining with the digoxigenin-labeled *abl* cDNA probes (B, D, F and I) or with anti-ablkin (K, M, O, Q and S). (A) High levels of *abl* mRNA were detected in stage 1 wild-type embryos. (C, E) The intensity of staining remained relatively unchanged through cellularization of the blastoderm (C, mid stage 2 embryo and E, cellular blastoderm). (G) During early gastrulation, the level of staining for *abl* mRNA decreased. (H,I) By germ band extension, the staining levels in wild-type (H) and maternal *abl* null embryos (I) were indistinguishable. (J) In contrast to the presence of *abl* mRNA at the earliest stages, stage 1 embryos did not contain detectable levels of abl protein. Arrowheads in J indicate positions of the embryonic nuclei following the second mitosis. (L) abl protein was detected in stage 2, above the background level of staining observed in the maternal *abl* null embryos. Staining for abl was associated with the energids around the precellular nuclei (arrowheads in L and M). (N, P, R) At cellular blastoderm and during germband extension, abl was detected throughout the embryo. In contrast to the decline in staining for abl mRNA at the later stages, the intensity of the immunostaining did not change.

nuclear division (compare Fig. 2J, wild type, with Fig. 2K, *abl* null). At this stage cytoplasmic islands, energids, form around the nuclei in the anterior end of the embryo (arrowheads in Fig. 2J; Campos-Ortega and Hartenstein, 1985). A detectable level of abl protein was first observed after the fourth nuclear division (stage 2). The protein was distributed throughout the embryos (compare Fig. 2L with Fig 2M). The intensity of anti-ablkin staining increased through the remaining nuclear cleavage cycles to the onset of gastrulation (Fig. 2N,P). The level of abl, as detected by anti-ablkin, remained constant throughout gastrulation and early germ band extension (Fig. 2R). Embryos produced from *abl* null mothers did not stain with anti-ablkin at these stages (Fig. 2K,M,O,Q and S). Perdurance of the abl protein through gastrulation and germ band extension was in contrast to the decrease in the level of the maternal *abl* mRNA (compare Fig. 2P,R with G,H). Staining of abl protein derived from the maternal message was detected through full germ band extension (data not shown).

The subcellular localization of the abl protein during these early stages of embryogenesis was examined in sections through cellularizing and gastrulating embryos. The abl protein in precellular embryos was detected throughout the energids and cortical regions, but was concentrated near the plasma membrane (Fig. 3A, arrows). At the onset of cellularization, cleavage furrows formed between the peripheral nuclei of the embryo. Immunostaining for the abl protein was concentrated near the cleavage furrows (Fig. 3B, arrows) and remained associated with the furrows as they progressed inward (Fig. 3C, arrows). The highest level of immunostaining for the abl protein was concentrated at cell junctions in the apical region of the cells through the completion of cellularization (Fig. 3D, arrows). This localization to the plasma membrane was transient; by early gastrulation the immunostaining for the abl protein was detected more diffusely throughout the apical cytoplasm (Fig. 3E), and in germ band extended embryos, the staining for the abl protein was diffuse throughout the cytoplasm of all cells in the ectoderm and mesoderm (Fig. 3F).

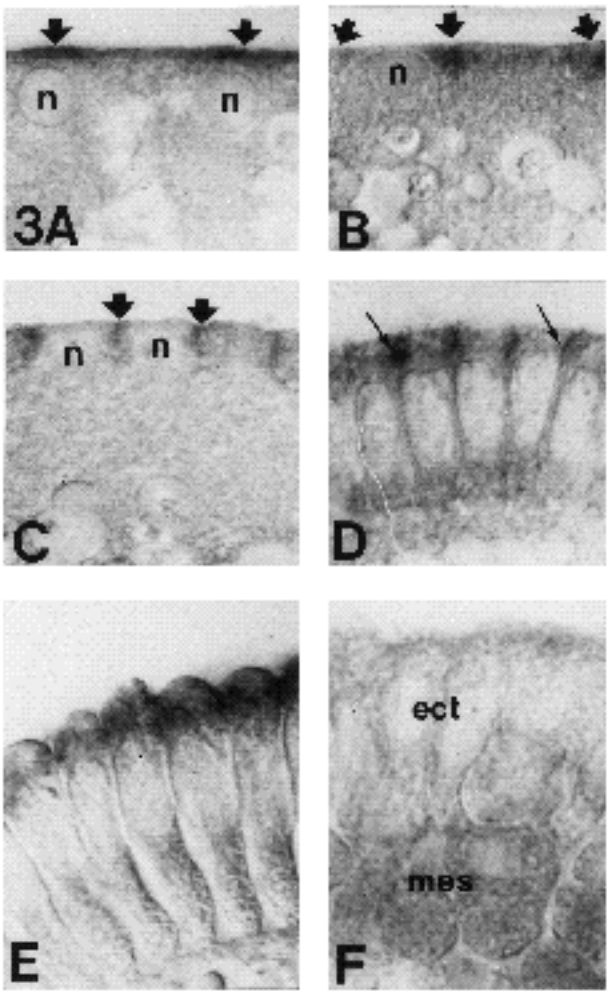

Fig. 3. Localization of abl protein to the cleavage furrows and apical cell junctions of cellularizing embryos. 6 μm sections were cut through wild-type embryos stained with anti-ablkin (as shown in Fig. 2). Dorsal surfaces are shown for A-E. In F, the ventral ectoderm is at the top and the mesoderm is at the bottom. In all cases the apical surface of the ectoderm is to the top. (A) At syncytial blastoderm, the highest level of abl immunostaining was at the plasma membrane with more intense staining (arrows) observed above the nuclei (n). (B,C) During the early phases of cellularization, abl was detected in the cleavage furrows (arrows) as they formed and protruded inwards. (D) At cellular blastoderm, abl immunostaining was concentrated in the apical cell junctions (arrows). (E) During early gastrulation (the ventral furrow had formed on the ventral surface of the embryo shown in this panel), abl was detected diffusely throughout the apical cytoplasm. (F) Although abl protein was detectable during germ band extension (Fig. 2R), the staining was diffuse throughout the entire cytoplasm at this stage (within both the mesoderm (mes) and ectoderm (ect)) and therefore not obvious in sections of embryos.

Expression of abl in the developing embryonic nervous system

We have previously reported that zygotic expression of the abl protein was detected in the axons of the developing central nervous system (CNS) of the *Drosophila* embryo (Gertler et al., 1989). The increased sensitivity of the anti-ablkin antibodies confirmed this observation and revealed a broader pattern of zygotic expression. Zygotic expression in the embryo was detected in the developing central nervous system and in the somatic and visceral musculature (Fig. 4). Embryos null for both maternal and zygotic abl protein expression were used to demonstrate that this immunostaining was specifically detecting abl protein (data not shown). After the completion of germ band extension (stage 11/12), immunostaining of zygotic abl protein was most intense in the neurons of the central nervous system (Fig. 4A). The tissue specificity of this early zygotic expression was masked by the ubiquitous perdurance of the maternal abl protein, therefore, the embryo shown in Fig. 4A was produced by a mother null for *abl*. Zygotic abl protein within the developing CNS was limited to the neurons; immunostaining was not detected in the neuroblasts or ganglion mother cells (Fig. 4B). The abl protein was found concentrated in the axons as they extended from the neurons (small arrows in Fig. 4E,F). The highest level of immunostaining throughout embryogenesis was observed in the axon scaffold of the CNS. As we have previously reported, immunostaining became stronger in the longitu-

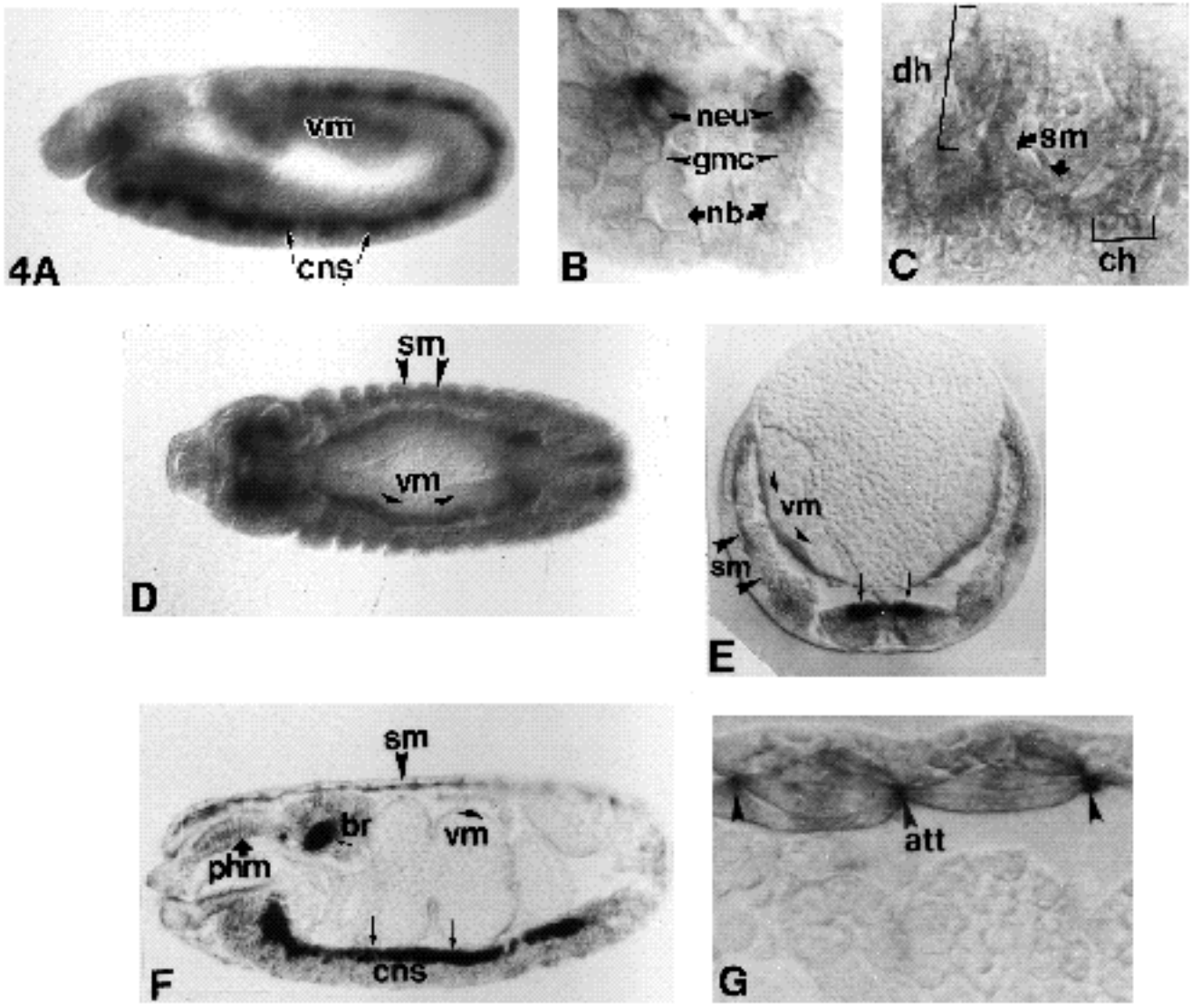

Fig. 4. Zygotic expression of the abl protein. Embryos were fixed and stained with anti-ablkin. Embryos are shown dorsal up and anterior to the left. (A) A lateral view of an early stage 12 embryo produced by an *abl* null mother and bearing an *abl*$^{+}$ paternally inherited chromosome. Early zygotic expression of abl was detected in the neurons of the CNS and in the visceral mesoderm (vm). (B) A transverse 6 μm section through a stage 12 embryo from an *abl* null mother similar to the embryo shown in A. Zygotic expression of abl in the CNS was not detected in the neuroblasts (nb) or ganglion mother cells (gmc), but was detected in the neurons (neu). (C) A parasagittal 6 μm section through a stage 16 embryo. Expression of abl was detected in the neurons of the PNS (dh, dorsal hair neurons; ch, chordotonal neurons; sm, somatic muscles). (D) A horizontal optical section through a stage 14 embryo. This view shows abl expression in the visceral mesoderm (vm) and the somatic mesoderm (sm). (E) A transverse 6 μm section of a stage 14 embryo. abl protein was detected in the visceral (vm) and somatic mesoderm (sm) and in the axons of the CNS (small arrows). (F) In a sagittal section through a stage 16 embryo, abl was detected in the axons of the CNS (small arrows; br, brain), in the visceral and somatic muscles and in the pharyngeal muscles (phm). (G) In a horizontal section through a stage 16 embryo, abl immunostaining in the somatic muscles was most intense at the muscle attachment sites (att).

dinal connectives than in the commissures (data not shown). In sagittal sections of stage-16 embryos it was clear that the abl protein was not restricted to CNS neurons, as faint staining for the abl protein could be detected with anti-ablkin in the neurons of the peripheral nervous system (PNS; Fig. 4C).

Expression of abl during embryonic muscle development

The mesodermal precursor cells undergo three rounds of cell divisions during germ band extension with the third mitosis at the end of stage 10 (Hartenstein and Campos-Ortega, 1985). This mitosis leads to the disruption of the mesodermal epithelium, separating the mesoderm into two layers which form the visceral and somatic musculature (stage 11/12; Campos-Ortega and Hartenstein, 1985). It is at this stage that zygotic abl protein can be detected in the developing mesoderm (Fig. 4A). By stage 14, expression of abl protein was readily detected in the visceral meso-

derm and faintly detected in the somatic mesoderm in both whole-mount embryos (Fig. 4D) and cross sections (Fig. 4E). The abl protein was detected in the mesoderm cells as they differentiated to form the visceral and somatic musculature (Fig. 4F). In the somatic muscle, immunostaining for the abl protein was concentrated at the muscle attachment sites (Fig. 4G). In later, stage 17, embryos, abl protein staining was no longer observed in the visceral or somatic muscle (data not shown).

Mutations in abl *and* dab *affect the stability of somatic muscles*

We have previously shown that embryos mutant for *abl* do not show overt embryonic mutant phenotypes and survive to pharate adult and adult stages (Henkemeyer et al., 1987). However, in the absence of one or both copies of *disabled* (*dab*), the axon scaffold of the CNS is disrupted, although no mutant phenotypes were observed in the PNS or the epidermis (Gertler et al., 1989). The observation that the abl protein was expressed in the developing muscles led us to look for mutant phenotypes in the muscle. Dr Rachel Drysdale (Cambridge University, Cambridge, UK) analyzed effects of mutations in *abl* and *dab* on embryonic muscle formation for us using polarized light microscopy (Broadie and Bate, 1991). She observed defects only in *abl dab* double mutant embryos; the presence of a single copy of *abl* or *dab* alleviated the majority of muscle defects. We examined the mutant phenotype of *abl dab* double mutant embryos using antibodies against myosin. Mutant embryos were selected for study as described in the methods. Of 15 mutant embryos examined at stage 15 (as determined by the morphology of the gut), only one exhibited a musculature defect (data not shown). In contrast, 13 of 15 embryos examined at late stage 16 had obvious defects in the somatic musculature (compare Fig. 5A,B with C,D). In the mutant embryos, many muscle fibers were absent, and those that remained were often thin and disorganized. In place of the missing fibers were round balls, possibly remnants of muscle fibers that detached from the epidermis.

abl expression in the larval and pupal imaginal disks

Mutations in *abl* result in reduced adult viability. The results of our studies on the expression of the *abl* gene in the embryo and the phenotypes of embryos mutant for both *abl* and *dab*, indicated that the reduction in adult viability might be due to disruptions in the development or function of the adult nervous system and musculature. Therefore, we examined the expression pattern of abl protein during late larval and early pupal development when the adult structures were being formed.

Many adult cuticular structures are derived from the larval imaginal disks. Since *abl* mutant flies do not have

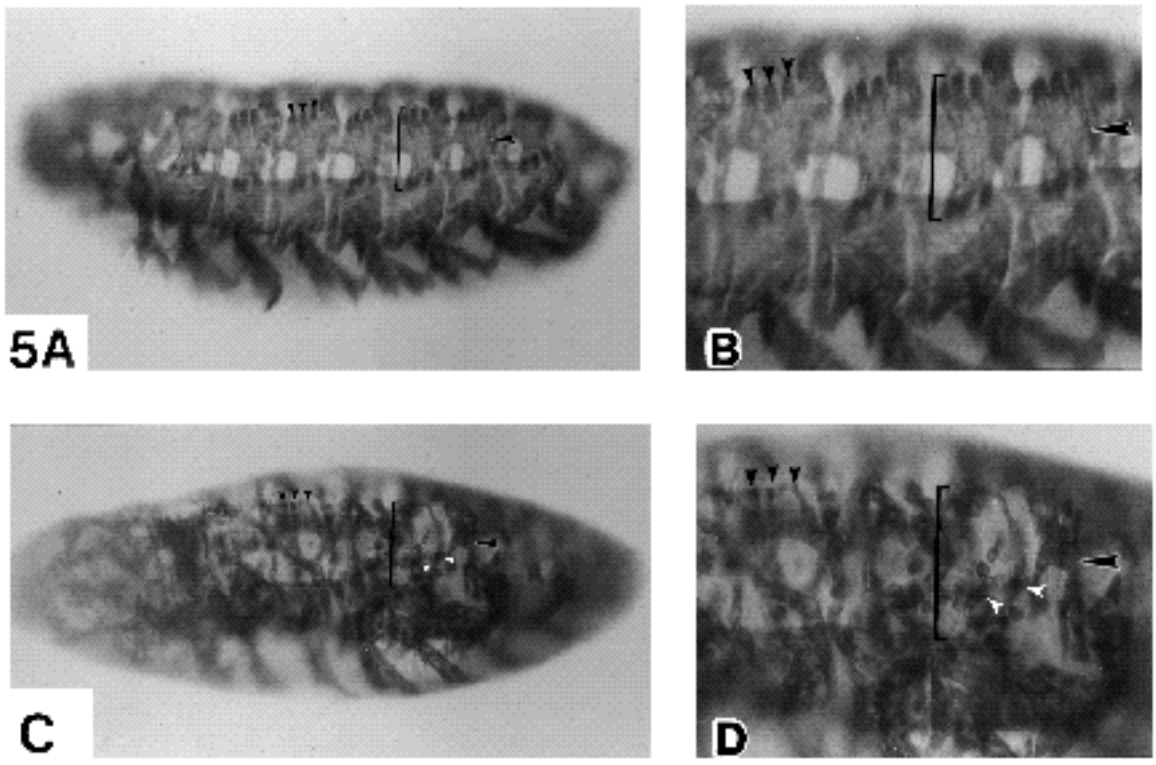

Fig. 5. Muscle defects associated with *abl dab* double mutant embryos. Ventral lateral views are shown of wild-type (A,B) and *abl dab* double mutant (C,D) embryos at stage 16 stained with an antibody against myosin to reveal the somatic musculature. (A,B) The regular structure of the embryonic musculature in wild-type embryos was observed. The muscles were highly organized and thick. (C,D) In the *abl dab* double mutant embryos, the muscles were disorganized and often absent. Compare the bracketed regions of A and B with those of C and D. The ends of the muscle were not as broad as in wild type (small black arrowheads) and the muscles were often thin (large black arrowhead). In place of some muscles were irregular balls that stained with the myosin antibody; these balls were often connected by thin cytoplasmic bridges (white arrowheads).

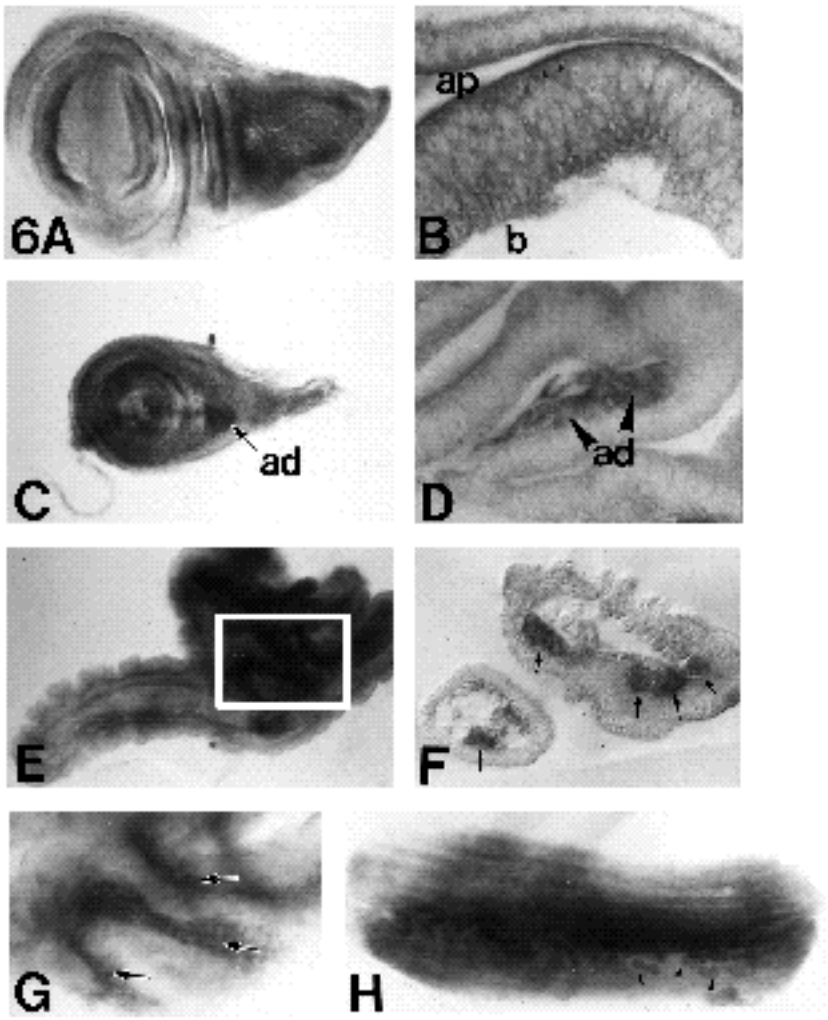

Fig. 6. Expression of abl in the imaginal disks and developing muscles in third instar larvae and pupae. Imaginal disks were dissected from late third instar larvae and 6 hour ppf pupae and stained with anti-ablkin. (A) abl protein was detected in the epithelial cells of the third instar wing imaginal disks. (B) In 6 μm sections through a wing disk there was an increased intensity of abl immunostaining in the apical (ap) cortical region of the epithelial cells (b, basal). (C) Third instar leg imaginal disks had, in addition to the general staining of the disk epithelium, patches with higher levels of abl immunostaining in regions containing adepithelial cells (ad). (D) 6 μm sections through leg imaginal disks showed that the increased levels of staining in these regions of the leg imaginal disk were contained in the adepithelial cells rather than the disk epithelium. (E) 6 hour ppf everting leg imaginal disks had increased levels of abl immunostaining in adepithelial (muscle precursor) cells of the developing notum. A detail of the boxed region in E is shown in G (arrows point to bundles of abl expressing cells). (F) A cross section through a 6 hour ppf leg imaginal disk showed that the increased staining for the abl protein was not in the epithelial cells, but was restricted to cells forming the adult thoracic muscles. (H) The abl protein was detected in both the maturing muscle fibers and in the unfused myoblasts (arrowheads) in indirect flight muscles dissected from 27 hour ppf pupae.

cuticular defects outside of the eye (discussed below), we did not expect to find abl protein generally expressed in the imaginal disks. However, abl protein was detected in the epithelial cells of all imaginal disks examined (leg, wing, and eye-antennal; Figs 6A,C, 7A). The level of staining observed in these cells was consistently lower than the level observed in developing neurons and muscle (discussed below). That this low-level staining resulted from detection of the abl protein was confirmed by staining imaginal disks dissected from abl protein null larvae and pupae with anti-ablkin (data not shown). The abl protein was present throughout the cytoplasm, but was concentrated within the apical cortical region of the cells (Fig. 6B), a region containing actin-rich adherens-type junctions (Poodry and Schneiderman, 1970).

In addition to the epithelial sheet of cells, the imaginal disks contain groups of cells outside the epithelium, the adepithelial cells. These cells give rise to much of the musculature of the adult thorax (Poodry and Schneiderman, 1970; Reed et al., 1975; Ursprung et al., 1972; Bate et al., 1991). In wing and leg imaginal disks, there were patches of immunostaining for the abl protein that were more intense than the general staining of the epithelial cells of the imaginal disks. This staining was most striking in the leg disk (Fig. 6C, arrow). Sections through a leg imaginal disk confirmed that this staining was in the adepithelial cells (Fig. 6D). In the leg imaginal disk, only the adepithelial cells that had migrated into the more distal folds of the leg pouch, and had begun morphological changes, showed an increased level of immunostaining for the abl protein.

In leg and wing disks dissected from 6 hour ppf pupae, there was a higher level of staining in the proximal region where the leg and wing imaginal disks had fused to form the notum (Fig. 6E,G). This higher level of staining was restricted to the cells adjacent to the basal surface of the disk epithelium (Fig. 6F). In whole-mount preparations, the pattern of staining with anti-ablkin was similar to that reported using the twist antibody, a marker for muscle precursor cells (Fernandes et al., 1991). By 27 hours ppf indirect flight muscle fibers were well formed as most of the myoblasts had fused to form the muscle fibers. At this stage, abl protein was detected in the muscle fibers as well as in the unfused myoblasts (Fig. 6H). In the larval and pupal stages studied, there was no detectable subcellular localization of the protein within the developing muscles. However, similar to the results in the embryo, the abl protein was present at increased levels in developing muscle cells.

Expression of abl during differentiation of the eye imaginal disk

The *Drosophila* eye consists of approximately 700 repeated simple eye units, or ommatidia. Differentiation of the eye imaginal disk from an unpatterned epithelium to a highly structured retina begins in the late third instar larvae when a morphogenetic furrow forms in the posterior end of the eye imaginal disk and moves toward the anterior end. Ahead of the furrow are mitotically active, unpatterned cells. Behind the furrow the cells become organized in a well established sequential pattern and begin neuronal differentiation (Tomlinson and Ready, 1987).

Low levels of abl protein expression were detected in undifferentiated cells ahead of the furrow (Fig. 7A). This level was similar to the level of immunostaining found in the epithelial cells of the leg and wing imaginal disks. Higher levels of abl immunostaining were detected in the developing photoreceptor cells (R-cells; Fig 7A), beginning approximately 3 rows behind the expression of the mAb22C10 antigen (Fig. 7C,D), a marker for neuronal differentiation of R-cells (Fujita et al., 1982; Tomlinson and Ready, 1987). The higher levels of abl protein were first detected simultaneously in R-cells 2, 5, and 8. The abl protein was then detected in the developing photoreceptor cells in the same order in which they had initiated neuronal differentiation within the developing ommatidial cluster: R-cells 3 and 4, followed by R-cells 1 and 6 and finally R-cell 7. The abl protein, though present throughout the photoreceptor cell bodies and axons, was concentrated in the apical portion of the cells (black arrow, Fig. 7C). abl was detected in the photoreceptor cells during the remaining stages of eye development examined (through 72 hours ppf). In the retina 27 hours ppf, higher levels of immunostaining were detected in all eight photoreceptor cells (Fig. 7E). Lower levels of staining were observed in the apical membranes of the accessory cells of the retina (Fig. 7F). By 72 hours ppf, abl protein was detected at higher levels in the neurons of the interommatidial bristles as well as the photoreceptor cells (Fig. 7G). Within the photoreceptor cells, the protein remained centrally localized and the staining extended into the forming rhabdomeres (Fig. 7H). Developing eye imaginal disks were dissected from *abl* null larvae and pupae and stained with anti-ablkin to demonstrate that the immunostaining observed in the eye was due to the expression of *abl* protein (Fig. 7B and data not shown).

Phenotype of abl *mutant eye*

Eyes of *abl* mutant adults were rough, have a slightly reduced number of facets, missing and supernumerary bristles, and facets irregular in shape and size (R.B., unpublished observations). Sections through *abl* mutant eyes reveal defects in all cell types of the retina: photoreceptor cells, cone cells and pigment cells (Henkemeyer et. al., 1987). These defects include a general lack of the hexagonal arrangement of ommatidia, missing and aberrantly oriented photoreceptor cells and rhabdomeres, and enlarged and dying pigment cells. Staining of *abl* mutant third instar eye imaginal disks with a monoclonal antibody against a neuronal specific form of neuroglian, mAbBP104 (Hortsch et al., 1990), revealed defects in the photoreceptor cell clusters early in ommatidial development (Fig. 7I,J). The initial establishment of photoreceptor patterning appeared to occur normally. No defects were detected in ommatidial spacing or the initial three and five cell staining patterns of mAbBP104, representing the establishment of the 5 cell precluster and the neuronal differentiation of R-cells 2, 3, 4, 5 and 8. However, by row 6, when R-cells 1 and 6 were detected with mAbBP104, abnormal clusters were seen. At this stage, some clusters in the *abl* mutant eye imaginal disks had lost their symmetrical organization and contained extra cells expressing the mAbBP104 antigen, indicating a breakdown in the regulation of differentiation in the mutant ommatidia.

Fig. 7. Expression of abl protein and *abl* mutant phenotype during eye development. Larval and pupal eye disks were dissected and stained with anti-ablkin. (A) abl was detected in all cells of the third instar eye imaginal disk. However, the level of the abl immunostaining was higher in the differentiating photoreceptor cells posterior to the morphogenetic furrow (arrowhead marks the position of the morphogenetic furrow; ant, anterior; os, optic stalk). (B) Third instar eye imaginal disks from *abl* null larvae were stained with anti-ablkin to control for background levels of staining. Note that the non-photoreceptor cell staining in A was above the background levels of staining in B. (C) Confocal image of a third instar eye imaginal disk doubly stained with anti-ablkin (green) and mAb22C10 (red); regions of strong overlap appear yellow. Rows are numbered relative to the first row in which mAb22C10 staining was observed in R-8 (white arrow). A schematic of the image shown in C is shown in D. The increased intensity of abl immunostaining in the photoreceptor cells was detected simultaneously in R-cells 2, 5 and 8 in row 4 (note bracketed cluster in row 4). By row 8 mAb22C10 immunostaining was detected in R-cells 1, 2, 3, 4, 5, 6 and 8 (note bracketed cluster in row 8), however abl immunostaining was detected only in R-cells 2, 3, 4, 5 and 8, not in R-cells 1 and 6. Like mAb22C10 antigen, abl is concentrated at the apical regions of the photoreceptor cell clusters (indicated by arrowhead pointing to cluster edge of eye disk in row 8). (E) A 27 hour ppf eye. abl protein is detected in all eight photoreceptor cells. (F) A 4 μm radial section showing the detection of abl protein in the developing accessory cells. The protein was concentrated near the apical membranes (a, apical; b, basal). (G) In an apical optical section (72 hours ppf), abl was detected in the neurons of the interommatidial bristles (arrowheads) and the photoreceptor cells. (H) The staining for abl protein extended into the rhabdomeres of the photoreceptor cells (small arrow). (I) Defects in ommatidial development could be seen in the third instar eye imaginal disk stained with mAbBP104. A schematic of I is shown in J. Photoreceptor cell clusters appeared wild type through the initial establishment of the 5 cell staining pattern of mAbBP104 (row 4 of mAbBP104 antigen expression). By row 6, abnormal clusters (plain brackets) could be seen interspersed with normal clusters (starred brackets). Cells expressing mAbBP104 antigen were identified by their position within the developing clusters; cells that could not be identified are labeled with question marks.

abl expression in the developing adult nervous system

Sensory neurons in the imaginal disks differentiate during late larval and early pupal development (Hartenstein and Posakony, 1989). Wings dissected from 6 hour ppf pupae had, in addition to the general immunostaining observed in early wing disks with the anti-ablkin antibody, strong immunostaining of the early neurons of the wing blade that

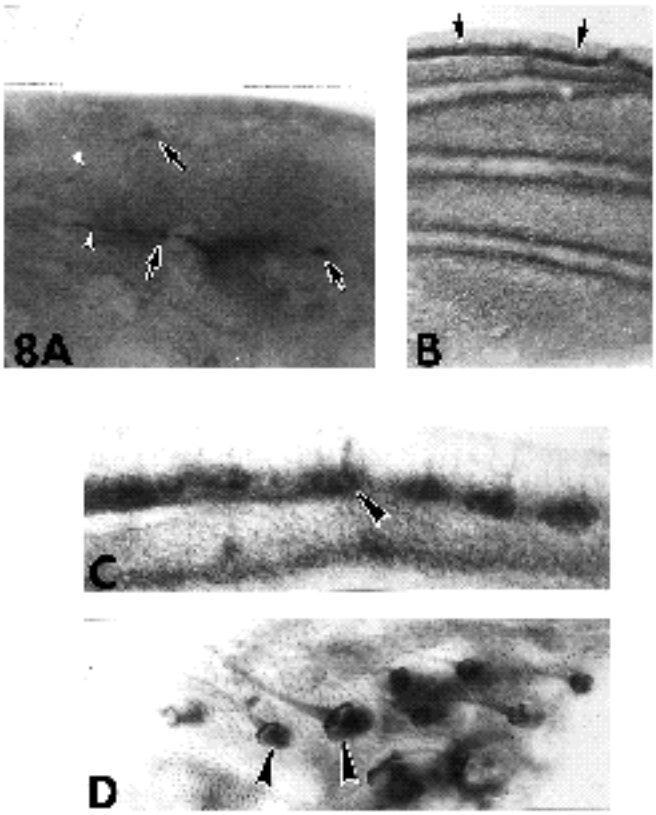

Fig. 8. Expression of abl in the neurons of the adult sensory bristles. Differentiating wing disks were dissected from staged pupae and stained with anti-ablkin. (A) In the 6 hour wing disk, abl was detected in all cells of the developing wing blade but at higher levels in the cell bodies (black arrows) and axons (white arrowheads) of the early differentiating neurons. (B) In the 27 hour wing disk, higher levels of abl were detected in the cell bodies and axons of the triple row sensory bristle neurons along the anterior wing margin (arrows). A higher resolution view of these neurons along the anterior wing margin of a 27 hour ppf wing is shown in C. Increased staining was also present in stripes on the wing blade that appear to delineate the wing veins. (D) Immunostaining of the neurons of the vertical and post-orbital bristles (arrowheads) observed in heads dissected from 72 hour ppf head and stained with anti-ablkin.

form along the presumptive third wing vein, L3 (Fig. 8A, black arrows) The staining was detected in the axons extended along L3 (white arrowheads in Fig. 8A). Later in development, at 27 hours ppf, the triple row and double row bristle neurons along the anterior wing margin stained intensely with anti-ablkin (Fig. 8B,C). Staining was detected in both the cell bodies and axons. Increased staining was also detected along the presumptive wing veins but this was not examined in any further detail. Neither the general nor the neuronal specific staining was present in abl protein-null wings (data not shown). Staining could also be seen in the bristle neurons of the notum at this time (data not shown) and the vertical and post-orbital bristles around the eye (Fig. 8D).

In addition to the neurons of the sensory bristles and the eye, *abl* protein was detected in the neurons of the developing adult CNS (Fig. 9). By late third instar, the axons of the larval neurons, which were formed during embryogenesis, no longer expressed detectable levels of abl protein, but staining was observed in the neurons that were forming the adult CNS (Fig. 9A). As in the embryo, abl protein was not detected in the neuroblasts, but was restricted to their progeny, the neurons of the adult CNS (Fig. 9B). Sections through the nerve cord and brain of a 6 hour ppf pupa stained with anti-ablkin revealed that the *abl* protein was present in the developing neuropil (Fig. 9C,D).

Discussion

abl protein levels increase transiently in post-mitotic differentiating cells

abl is expressed in a variety of tissues during several stages of *Drosophila* development. Aside from the levels of abl protein supplied to the early embryo by maternally provided *abl* mRNA, the highest levels of abl protein are achieved in differentiating neurons and muscles during both embryogenesis and pupation. In the embryonic CNS, this increase in abl protein level does not occur in the proliferating cells of the neural cell lineage, the neuroblasts and ganglion mother cells, but in the post-mitotic neurons as they begin axonogenesis. Similarly, increased levels of abl protein occur in embryonic post-mitotic muscle development. In the developing eye imaginal disk, the delay between neural differentiation and increased levels of abl protein expression can be more clearly distinguished: the photoreceptor cells begin expressing higher levels of abl protein approximately 6 hours after they begin expressing neural antigens.

Although abl protein is present at higher levels in differentiating nerve and muscle cells, the level of abl protein falls after these tissues complete development. This observation is consistent with northern analyses, which indicate higher levels of *abl* expression during late embryogenesis and mid-pupation, times of neural and muscle development (Telford et al., 1985). We propose, therefore, that increased levels of abl protein may be involved in proper neural and muscle development, but are probably not necessary for nerve or muscle function. This is analogous to proposals regarding the function of c-*src* during vertebrate neuronal development. The level of $pp60^{c\text{-}src}$ in the nervous system is lower in adults than in embryos (Maness, 1988). However, if adult nerves are damaged, higher levels of $pp60^{c\text{-}src}$ reoccur in neurons and growth cones in the damaged region as the nerve regenerates, consistent with a requirement for increased tyrosine phosphorylation in neuronal differentiation and axonogenesis (Ignelzi et al., 1992).

abl protein is localized to specialized regions of cell-cell contact

Perhaps the most intriguing aspect of abl protein localization is the finding that the abl protein is asymmetrically distributed in most of the cells in which it is detected and is concentrated at specialized regions of cell-cell interaction. This is most apparent in the embryonic CNS where abl is highly concentrated in the axons relative to the cell bodies. In addition, the abl protein is concentrated at the muscle

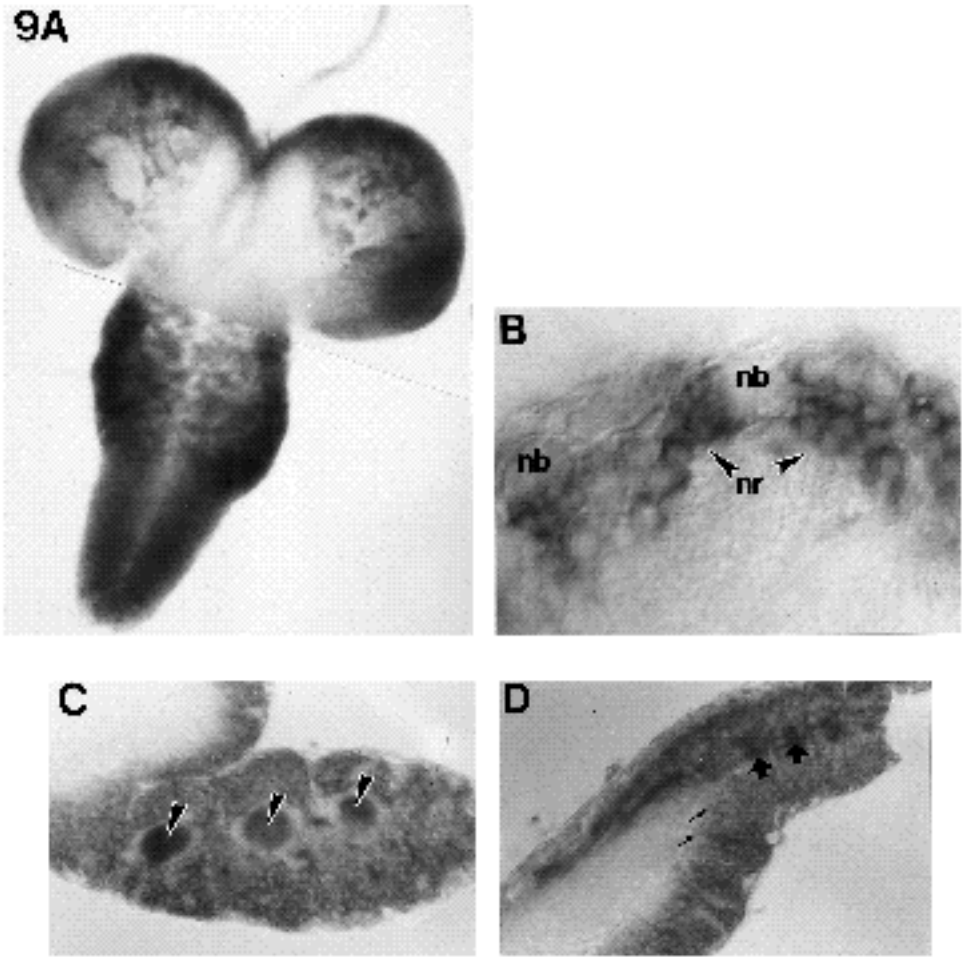

Fig. 9. Expression of abl in the neurons and neuropil of the developing adult central nervous system. CNS complexes from third instar and 6 hour ppf pupae were dissected and stained with anti-ablkin. (A) abl was detected in neurons of the third instar brain and ventral ganglia. (B) abl was detected at higher levels in neurons (nr) than in the neuroblasts (nb). (C,D) In the thoracic (C) and abdominal (D) ganglia of 6 hour ppf pupae, abl protein was detected in the axons extending toward (small arrows in D) and within (arrowheads in C and large arrows in D) the neuropil.

attachment sites in the embryo, and at apical cell junctions in both the blastoderm embryo and the imaginal disks. In the blastoderm embryo, the apical junctions are primarily desmosomes, adhesive junctions that are proposed to regulate the invagination of the plasma membrane during cellularization of the blastoderm (Campos-Ortega and Hartenstein, 1985). In the larval imaginal disks, the apical cell junctions are adherens and septate junctions (Poodry and Schneiderman, 1970). Adherens junctions are believed to be involved in tissue morphogenesis through their interactions with both actin and cell adhesion molecules (Tsukita et al., 1991) and are rich in phosphotyrosine containing proteins (Takata and Singer, 1988). The major protein components of adherens junctions, actin, α-actinin, talin, vinculin and integrins, are also major components of axonal growth cones and at the muscle attachment sites (Kellie, 1988; Sobue, 1988; Volk et al., 1990; Fyrberg et al., 1990). The localization of *Drosophila* abl to these structures indicates that the PTK may play some role in the regulation of these specialized cytoskeletal structures in several tissues.

Elimination of redundant processes reveals roles for abl in neural and muscle development

Null mutations in *abl* alone do not result in detectable phenotypes in the embryonic CNS or musculature. The development of these tissues in an *abl* mutant background, however, becomes sensitized to further genetic insults such that dominant genetic enhancer mutations have been recovered (Hoffmann, 1991). The genes in which the dominant genetic enhancer mutations map, e.g., the *dab* gene, may encode proteins that are functionally redundant to the abl PTK. While the molecular mechanisms for this functional compensation are not yet understood, the mutations in the enhancer genes have allowed the observation of tissue-specific developmental roles for the abl PTK in tissues that express transient, high levels of subcellularly localized abl protein.

In *abl dab* double mutant embryos, axons do not properly fasciculate to form commissures or longitudinal connectives, consistent with a role for the abl PTK in axonal outgrowth or for the proper intercellular adhesion required during axonal pathfinding (Gertler et al., 1989). In this paper we report that *abl dab* double mutant embryos also exhibit defects in embryonic muscle structure late in development. At earlier times in development, the muscle structure of *abl dab* double mutant embryos could not be distinguished from that of wild-type embryos. The late onset of the mutant phenotype within the developing muscles is consistent with failure of the muscle attachments as the muscles begin to twitch. This phenotype is similar to that reported for animals mutant for *lethal(1)myospheroid*

(Newman and Wright, 1981; Volk et al., 1990), which encodes the *Drosophila* β-integrin (MacKrell et al., 1988).

The eye is the only tissue in which we have scored morphological defects in simple *abl* mutant backgrounds but it should be noted that the eye phenotypes discussed in this paper can be rescued by a catalytically inactive abl protein (Henkemeyer et al., 1990). This phenotype and the poor adult viability of *abl* mutant flies, indicates that the abl protein has a non-catalytic structural role, perhaps bringing together other regulatory molecules in a multi-protein complex. We suspect that the catalytic role of the abl kinase activity in this complex is compensated for by dab or other gene products. With this caveat, we conclude from the observations reported here that abl is not involved in pattern formation within the eye imaginal disk, but is required for proper differentiation of retinal cells. The gross morphological defects in the adult eye may be due to additional requirements for *abl* in the brain or in the later development decisions in the eye, consistent with the continued expression of *abl* during pupal eye development. Examination of eye development in clones of cells mutant for both *abl* and *dab* may provide better insights about the role of the abl PTK in eye development.

All of the observed phenotypic consequences caused by *abl* mutations occur in tissues exhibiting transient increases in the level and subcellular localization of abl protein. However, the role of the abl PTK in these processes is largely redundant. The existence of compensatory regulatory mechanisms may be quite common in signal transduction and developmental processes such as those regulated by PTKs. *Drosophila* genetics provides an opportunity to identify and eliminate the compensatory mechanisms so that the developmental functions of PTKs and other highly conserved regulatory molecules can be studied.

We are grateful to Dr Rachel Drysdale for her help in studying the abl-dependent muscle phenotype and communications of her results, Dr Dan Woods for discussions regarding abl localization within imaginal disks and Dr Don Ready for discussions regarding the abl mutant eye phenotype. We thank Drs Daniel Kiehart, Corey Goodman and Tadmiri Venkatesh for gifts of antibodies. Drs Grace Panganiban and Carol Sattler provided technical advise for sectioning, Dr Stephen Paddock assisted with confocal microscopy and Jerry Sattler provided much needed photographic advise. We thank Drs Eric Liebl, Frank Gertler, and Grace Panganiban for thoughtful reading and comments on the manuscript. This work was supported by funding from the NIH including CA 49582 to F. M. H., Cancer Center Core support CA 07175 to H.C. Pitot and predoctoral training grant CA 09135 for support of R. L. B.; F. M. H. is the recipient of a Faculty Research Award from the American Cancer Society.

References

Adamson, E. D. (1987). Oncogenes in development. *Development* **99**, 449-471.

Bate, M., Rushton, E. and Currie, D. A. (1991). Cells with persistent *twist* expression are the embryonic precursors of adult muscles in *Drosophila. Development* **113**, 79-89.

Broadie, K. S. and Bate, M. (1991). The development of adult muscles in *Drosophila*: ablation of identified precursor cells. *Development* **113**, 103-118.

Campos-Ortega, J. A. and Hartenstein, V. (1985). *The Embryonic Development of* Drosophila melanogaster. Berlin, Heidelberg, New York, and Tokyo: Springer-Verlag.

Collett, M. S. and Erikson, R. L. (1978). Protein kinase activity associated with the avian sarcoma virus *src* gene product. *Proc. Natl. Acad. Sci.USA* **75**, 2021-2024.

Daley, G. Q. and Ben-Neriah, Y. (1991). Implicating the *bcr/abl* gene in the pathogenesis of Philadelphia chromosome-positive human leukemia. *Adv. Cancer Res.* **57**, 151-183.

Devereaux, J., Haeberli, P. and Smithies, O. (1984). A comprehensive set of sequence analysis programs for the VAX. *Nucl. Acids Res.* **12**, 387-395.

Elkins, T., Zinn, K., McAllister, L., Hoffmann, F. M. and Goodman, C. S. (1990). Genetic analysis of a *Drosophila* neural cell adhesion molecule: interaction of *fasciclin I* and Abelson tyrosine kinase mutations. *Cell* **60**, 565-575.

Fernandes, J., Bate, M., and Vijayraghavan, K. (1991). Development of the indirect flight muscles of *Drosophila*. *Development* **113**, 67-77.

Fujita, S. C., Zipursky, S. L., Benzer, S., Ferrus, A., and Shotwell, S. L. (1982). Monoclonal antibodies against the *Drosophila* nervous system. *Proc. Natl. Acad. Sci.USA* **79**, 7929-7933.

Fyrberg, E., Kelly, M., Ball, E., Fyrberg, C. and Reedy, M. C. (1990). Molecular genetics of *Drosophila* actin-actinin: mutant alleles disrupt Z-disks integrity and muscle insertions. *J. Cell Biol.* **110**, 1999-2011.

Gertler, F. B., Bennett, R. L., Clark, M. J. and Hoffmann, F. M. (1989). *Drosophila abl* tyrosine kinase in embryonic CNS axons: a role in axonogenesis is revealed through dosage sensitive interactions with *disabled*. *Cell* **58**, 103-113.

Gertler, F. B., Doctor, J. S. and Hoffmann, F. M. (1990). Genetic suppression of mutations in the *Drosophilaabl* proto-oncogene homolog. *Science* **248**, 857-860.

Hanley, M. R. (1988). Proto-oncogenes in the nervous system. *Neuron* **1**, 175-182.

Hartenstein, V. and Campos-Ortega, J. A. (1985). Fate mapping in wild type *Drosophila melanogaster* 1. The spatio-temporal pattern of embryonic cell division. *Roux's Arch. Dev. Biol.* **194**, 181-185.

Hartenstein, V. and Posakony, J. (1989). Development of adult sensilla on the wing and notum of *Drosophila melanogaster*. *Development* **107**, 389-405.

Henkemeyer, M. J., Bennett, R. L., Gertler, F. B. and Hoffmann, F. M. (1988). DNA sequence, structure, and tyrosine kinase activity of the *Drosophila* Abelson proto-oncogene homolog. *Mol. Cell. Biol.* **8**, 843-853.

Henkemeyer, M. J., Gertler, F. B., Goodman, W. and Hoffmann, F. M. (1987). The *Drosophila* Abelson proto-oncogene homolog: identification of mutant alleles that have pleiotropic effects late in development. *Cell* **51**, 821-828.

Henkemeyer, M., West, S. R., Gertler, F. B. and Hoffmann, F. M. (1990). A novel tyrosine kinase-independent function of *Drosophila abl* correlates with proper subcellular localization. *Cell* **63**, 949-960.

Hoffmann, F. M. (1991). *Drosophilaabl* and genetic redundancy in signal transduction. *Trends Genet.* **7**, 351-355.

Holland, G. D., Henkemeyer, M. J., Kaehler, D. A., Hoffmann, F. M. and Risser, R. (1990). Conservation of function of *Drosophila melanogaster abl* and murine *v-abl* proteins in transformation of mammalian cells. *J. Virology* **64**, 2226-2235.

Hortsch, M., Bieber, A., Patel, N. H. and Goodman, C. S. (1990). Differential splicing generates a nervous system-specific form of *Drosophila* neuroglian. *Neuron* **4**, 697-709.

Hunter, T. and Sefton, B. M. (1980). Transforming gene product of Rouse sarcoma virus phosphorylates tyrosine. *Proc. Natl. Acad. Sci. USA.* **77**, 1311-1315.

Ignelzi, M. A. Jr., Padilla, S. S., Warder, D. E., and Maness, P. F. (1992). Altered expression of $pp60^{c\text{-}src}$ induced by peripheral nerve injury. *J. Comp. Neurol.* **315**, 171-177.

Johnson, D. A., Gautsch, J. W., Sportsman, J. R. and Elder, J. H. (1984). Improved technique utilizing nonfat dry milk for analysis of proteins and nucleic acids transferred to nitrocellulose. *Gene Analyt. Technol.* **1**, 3-8.

Kellie, S. (1988). Cellular transformation, tyrosine kinase oncogenes, and the cellular adhesion plaque. *Bioessays* **8**, 25-30.

Kruh, G. D., Perego, R., Miki, T. and Aaronson, S. A. (1990). The complete coding sequence of *arg* defines the Abelson subfamily of cytoplasmic tyrosine kinases. *Proc. Natl. Acad. Sci.USA* **87**, 5802-5806.

Laemmli, U. K. (1970). Cleavage of structural proteins during the assembly of the head of bacteriophage T4. *Nature* **227**, 680-685.

MacKrell, A. J., Blumberg, B., Haynes, S. R. and Fessler, J. H. (1988). The lethal myospheroid gene of *Drosophila* encodes a membrane protein homologous to vertebrate integrin-β subunits. *Proc. Natl. Acad. Sci.USA* **85**, 2633-2637.

Maness, P. F., Aubry, M., Shores, C. G., Frame, L. and Pfenninger, K. H. (1988). c-*src* gene product is enriched in nerve growth cone membranes. *Proc. Natl. Acad. Sci.USA* **85**, 5001-5005.

Masucci, J. D., Miltenberger, R. J. and Hoffmann, F. M. (1990). Pattern-specific expression of the *Drosophila decapentaplegic* gene in the imaginal disks is regulated by 3′ *cis*-regulatory elements. *Genes Dev.* **4**, 2011-2023.

Nagai, K., Perutz, M. F. and Poyart, C. (1985). Oxygen binding properties of human mutant hemoglobins synthesized in *Escherichia coli. Proc. Natl. Acad. Sci.USA* **82**, 7252-7255.

Newman, S. M. Jr. and Wright, T. R. F. (1981). A histological and ultrastructural analysis of developmental defects produced by the mutation, *lethal(1)myospheroid*, in *Drosophila melanogaster. Dev. Biol.* **86**, 393-402.

Perego, R., Ron, D. and Kruh, G. D. (1991). *Arg* encodes a widely expressed 145 kDa PTK. *Oncogene* **6**, 1899-1902.

Poodry, C. A. and Schneiderman, H. A. (1970). The ultrastucture of the developing leg of *Drosophila melanogaster. Wilhelm Roux' Arch. devl. Biol.* **166**, 1-44.

Reed, C. T., Murphy, C. and Fristrom, D. (1975). The ultrastructure of the differentiating pupal leg of *Drosophila melanogaster. Wilhelm Roux' Arch. devl. Biol.* **178**, 285-302.

Schwartzberg, P. L., Stall, A. M., Hardin, J. D., Bowdish, K. S., Humaran, T., Boast, S., Harbison, M. L., Robertson, E. J. and Goff, S. P. (1991). Mice homozygous for the *abl*^{m1}mutation show poor viability and depletion of selected B and T cell populations. *Cell* **65**, 1165-1175.

Sobue, K. (1990). Involvement of the membrane cytoskeletal proteins and the *src* gene product in growth cone adhesion and movement. *Neuroscience Res.* Suppl. **13**, 80-91.

Takata, K. and Singer, S. J. (1988). Phosphotyrosine-modified proteins are concentrated at the membranes of epithelial cells during tissue development in chick embryos. *J. Cell Biol.* **106**, 1757-1764.

Tautz, D. and Pfeiffle, C. (1989). A non-radioactive *in situ* hybridization method for the localization of specific RNAs in *Drosophila* reveals translational control of the segmentation gene *hunchback. Chromosoma* **98**, 81-85.

Telford, J., Burckhardt, J., Butler, B. and Pirrota, V. (1985). Alternative processing and developmental control of the transcripts of the *Drosophila abl* oncogene homolog. *EMBO J.* **4**, 2609-2615.

Tomlinson, A. and Ready, D. F. (1987). Neuronal differentiation in the *Drosophila* ommatidium. *Dev. Biol.* **120**, 366-376.

Tsukita, S., Oishi, K., Akiyama, T., Yamanashi, Y., Yamamoto, T. and Tsukita, S. (1991). Specific proto-oncogenic tyrosine kinases of src family are enriched in cell-to-cell adherens junctions where the level of tyrosine phosphorylation is elevated. *J. Cell Biol.* **113**, 867-879.

Tybulewicz, V. L. J., Crawford, C. E., Jackson, P. K., Bronson, R. T. and Mulligan, R. C. (1991). Neonatal lethality and lymphonemia in mice with a disruption of the c-*abl* proto-oncogene. *Cell* **65**, 1153-1163.

Ursprung, H., Concience-Egli, M., Fox, D. and Walliman, T. (1972). Origin of leg musculature during Drosophila metamorphosis. *Proc. Natl. Acad. Sci.USA* **69**, 2812-2813.

Volk, T., Fessler, L. I., and Fessler, J. H. (1990). A role for integrin in the formation of sarcomeric cytoarchitecture. *Cell* **63**, 525-536.

Wadsworth, S. C., Madhaven, K. and Bilodeau-Wentworth, D. (1985). Maternal inheritance of transcripts from three *Drosophila src*-related genes. *Nucl. Acids Res.* **13**, 2153-2170.

Witte, O. N. (1986). Functions of the *abl* oncogene. *Cancer Surveys* **5,** 183-197.

Witte, O. N., Dasgupta, A., and Baltimore, D. (1980). Abelson murine leukemia virus protein is phosphorylated in vitro to form phosphotyrosine. *Nature* **283**, 826-831.

(Accepted 28 August 1992)